Ras Regulation by Reactive Oxygen and Nitrogen Species

Jongyun Heo[‡] and Sharon L. Campbell*[,‡,§]

Department of Biochemistry and Biophysics, University of North Carolina, 530 Mary Ellen Jones Building, Chapel Hill, North Carolina 27599-7260, and Lineberger Comprehensive Cancer Center, University of North Carolina at Chapel Hill, Chapel Hill, North Carolina 27599

Received September 14, 2005; Revised Manuscript Received November 22, 2005

ABSTRACT: Ras GTPases cycle between inactive GDP-bound and active GTP-bound states to modulate a diverse array of processes involved in cellular growth control. We have previously shown that both NO/O_2 (via nitrogen dioxide, $^{\cdot}NO_2$) and superoxide radical anion ($O_2^{\cdot-}$) promote Ras guanine nucleotide dissociation. We now show that hydrogen peroxide in the presence of transition metals (i.e., H_2O_2/transition metals) and peroxynitrite also trigger radical-based Ras guanine nucleotide dissociation. The primary redox-active reaction species derived from H_2O_2/transition metals and peroxynitrite is $O_2^{\cdot-}$ and $^{\cdot}NO_2$, respectively. A small fraction of hydroxyl radical ($OH^{\cdot}$) is also present in both. We also show that both carbonate radical ($CO_3^{\cdot-}$) and $^{\cdot}NO_2$, derived from the mixture of peroxynitrite and bicarbonate, facilitate Ras guanine nucleotide dissociation. We further demonstrate that NO/O_2 and $O_2^{\cdot-}$ promote Ras GDP exchange with GTP in the presence of a radical-quenching agent, ascorbate, or NO, and generation of Ras-GTP promotes high-affinity binding of the Ras-binding domain of Raf-1, a downstream effector of Ras. S-Nitrosylated Ras (Ras-SNO) can be formed when NO serves as a radical-quenching agent, and hydroxyl radical but not $^{\cdot}NO_2$ or $O_2^{\cdot-}$ can further react with Ras-SNO to modulate Ras activity *in vitro*. However, given the lack of redox specificity associated with the high redox potential of $OH^{\cdot}$, it is unclear whether this reaction occurs under physiological conditions.

$p21^{Ras}$ (Ras), a founding member of the Ras superfamily of GTPases, cycles between inactive GDP-bound and active GTP-bound forms to modulate the association with regulators and downstream targets. High-affinity interactions with downstream effectors are achieved via the interaction with the GTP-bound form rather than the GDP-bound form of Ras. This, in turn, leads to effector activation and stimulation of downstream signaling pathways, resulting in a wide array of biological responses including cellular growth, differentiation, and apoptosis (*1*, *2*). One of the best-characterized downstream effectors of Ras is the Raf-1 kinase, which upon binding to the active GTP-bound form of Ras, causes Raf-1 stimulation and activation of the MAP kinase cascade (*3*, *4*). Thus, efficient temporal regulation of Ras activity in response to various stimulatory and inhibition signals is dependent upon Ras GDP/GTP cycling.

Ras GDP/GTP cycling is modulated by various regulatory proteins and redox agents, which enhance the intrinsically slow rate of Ras guanine nucleotide dissociation and GTP hydrolysis (*1*, *5*, *6*). GTPase-activating proteins (GAPs) downregulate Ras activity by stimulating the intrinsically slow rate of GTP hydrolysis to populate Ras in its inactive GDP-bound form, whereas guanine nucleotide exchange factors (GEFs) and various redox agents upregulate the Ras function by promoting guanine nucleotide exchange (GNE) to generate the active GTP-bound state of Ras *in vivo* (*7*−*15*). The redox-active Ras cysteine (Cys^{118}) is located in the nucleotide-binding NKXD motif, where X is cysteine in H-, K-, and N-Ras (*16*, *17*). Several other Ras-related GTPases, in addition to Ras, that contain a redox-active NKCD motif are also redox-sensitive, and we have recently demonstrated that Rap1A and Rab3A are sensitive to redox regulation by various redox agents *in vitro* (*18*−*20*).

Two primary types of cellular redox agents have been identified to date and include both reactive nitrogen species (RNS) and reactive oxygen species (ROS). RNS include nitric oxide (NO), nitrogen dioxide ($^{\cdot}NO_2$, E_7 = ∼1.0 V versus NHE) (*21*), dinitrogen trioxide (N_2O_3), and peroxynitrite ($ONOO^-$) (*22*, 23). ROS include superoxide radical anion ($O_2^{\cdot-}$, E_7 = ∼0.9 V versus NHE) (*24*), perhydroxyl radical ($^{\cdot}OOH$; a protonated form of $O_2^{\cdot-}$), hydroxyl radical ($OH^{\cdot}$, E_7 = ∼2.3 V versus NHE) (*21*), and hydrogen peroxide (H_2O_2). Carbonate radical ($CO_3^{\cdot-}$, E_7 = ∼1.8 V versus NHE) (*21*) represents a reactive carbonated species that may also be present under physiological conditions (*23*). These RNS, ROS, and $CO_3^{\cdot-}$ are highly reactive and can react with each other, decompose, and be converted to other forms of RNS, ROS, and $CO_3^{\cdot-}$. For example, NO can react with O_2 to produce $^{\cdot}NO_2$, and $^{\cdot}NO_2$ can further react with NO to produce N_2O_3 (*22*). NO can also react with $O_2^{\cdot-}$ to produce $ONOO^-$, which, in turn, can be decomposed into $^{\cdot}NO_2$ and a small fraction of $OH^{\cdot}$ (*23*). $ONOO^-$ can further react with CO_2 to produce $CO_3^{\cdot-}$ and $^{\cdot}NO_2$ (*25*) with the rate of $^{\cdot}NO_2$ formation (as well as $CO_3^{\cdot-}$) from $ONOO^-$ in the presence of CO_2 faster than in the absence of CO_2 (*25*). Moreover, H_2O_2 can be converted into $O_2^{\cdot-}$, in the presence of transition metals (i.e., Cu^{2+} and Fe^{2+}) and O_2 at physio-

* To whom correspondence should be addressed. E-mail: campbesl@med.unc.edu. Fax: (919) 966-2852. Telephone: (919) 966-7139.

‡ Department of Biochemistry and Biophysics.

§ Lineberger Comprehensive Cancer Center.

10.1021/bi051872m CCC: $33.50
Published on Web 01/31/2006

logical pH. In this two-step reaction, the transition-metal-catalyzed Fenton reaction (*26*) converts H_2O_2 into $OH^{\cdot}$, $^{\cdot}OOH$, and OH^-. Moreover, $^{\cdot}OOH$ in the reaction mixture is most likely deprotonated to $O_2^{\cdot-}$, because the pK_a of $^{\cdot}$-OOH (~4.8) (*27*) is lower than physiological pH (i.e., pH 7.5). $O_2^{\cdot-}$ can be then be reconverted to $OH^{\cdot}$ and H_2O_2 by the transition-metal-catalyzed Harber−Weiss reaction (*28*).

NO is generated intracellularly by nitric oxide synthases (NOS), which catalyze the oxidation of L-arginine to NO and L-citrulline (*29*). However, when the substrate L-arginine is not present, NOS can produce $O_2^{\cdot-}$ (*30*). Despite the sizable interest in NOS as an NO-producing enzyme, several studies have implicated xanthine oxidase (XO) in production of NO (*31*, *32*). Although XO as well as cyclooxygenase (Cox2) mainly generate H_2O_2 (*33*, *34*), XO also produces $O_2^{\cdot-}$ (*35*). $O_2^{\cdot-}$ is also produced from the NADPH oxidase systems (*36*).

We have recently elucidated the mechanism by which NO/O_2 (via $^{\cdot}NO_2$) and $O_2^{\cdot-}$ promote Ras guanine nucleotide dissociation (*18*−*20*). The mechanism is fundamentally similar for both NO/O_2 and $O_2^{\cdot-}$, in that either $^{\cdot}NO_2$, a reaction product of NO with O_2, or $O_2^{\cdot-}$ reacts with the Ras-Cys^{118} thiol to produce a Ras-Cys^{118}-thiyl radical (Ras-Cys$^{118\cdot}$) intermediate (*18*−*20*). The Ras-Cys$^{118\cdot}$ then electronically interacts with Ras-bound GDP via the Phe^{28} side chain and initiates radical-based conversion of Ras-bound GDP into a Ras-bound GDP neutral radical (G$^{\cdot}$-DP) (*19*, *20*). Ras-bound G$^{\cdot}$-DP can further react with an additional $^{\cdot}NO_2$ or $O_2^{\cdot-}$ (whichever is available) to produce GDP−NO_2 (5-nitro-GDP) or GDP−O_2 (5-oxo-GDP), respectively (*19*, *20*). Although $^{\cdot}NO_2$ and $O_2^{\cdot-}$ facilitate nucleotide dissociation from Ras, nucleotide association does not occur in the absence of a radical-quenching agent, because further reaction of redox agents with the GDP-deficient (apo) Ras Cys^{118} thiol may produce apo Ras Cys$^{118\cdot}$, which results in the inhibition of Ras nucleotide (i.e., GTP) association. However, Ras guanine nucleotide association can be initiated by the addition of a radical-quenching agent (i.e., ascorbate), most likely because of the quenching of Ras radical intermediate(s) and thus facilitate $^{\cdot}NO_2$- or $O_2^{\cdot-}$-mediated Ras guanine nucleotide dissociation and association (i.e., Ras GNE) (*19*, *20*). If NO serves as a quenching agent by reacting with apo Ras Cys$^{118\cdot}$ in the presence of a nucleotide, the resultant reaction product is S-nitrosylated Ras (Ras-SNO) (*19*, *20*). However, it is unclear what role, if any, Ras-SNO plays in cells. While these mechanistic studies (*19*, *20*) focused on the molecular mechanism of $^{\cdot}NO_2$- and $O_2^{\cdot-}$-mediated Ras GNE, *in vitro* redox-mediated Ras activation via exchange of Ras-bound GDP with GTP (Ras GNE) was not demonstrated. Moreover, although our previous study demonstrated that $O_2^{\cdot-}$ but not H_2O_2 is effective in facilitating Ras guanine nucleotide dissociation (*20*), various oxidative agents (i.e., H_2O_2 and hemin) have been shown to enhance GNE on Ras *in vitro* and Ras-mediated mitogen-activated protein (MAP) kinase activity in Jurkat cells (*37*). Furthermore, Adachi et al. recently showed that H_2O_2-induced modification of Ras at Cys^{118} facilitates the activation of p38 and Akt but not extracellular signal-regulated kinase (ERK) in Rat vascular smooth muscle cells (*7*).

In this study, we have identified and characterized the redox-active species that facilitate H_2O_2/transition metals and $ONOO^-$-mediated Ras guanine nucleotide dissociation in the presence and absence of CO_2. In addition, the redox properties of S-nitrosylated Ras (Ras-SNO) are presented. The effect of redox agents on Ras GNE (GDP exchange for GTP) and binding interactions with the Ras-binding domain (RBD) of Raf-1 are also investigated to assess the action of redox agents *in vitro* under conditions that may mimic redox-mediated Ras-signaling processes observed *in vivo*.

EXPERIMENTAL PROCEDURES

Preparation of Chemicals. The chemicals used for all experiments were obtained from Sigma and of the highest grade unless otherwise noted. Radiolabeled guanine nucleotides ([^{3}H]GDP and [^{3}H]GTP) were obtained from Perkin Elmer Life Sciences. The radiolabeled guanine nucleotides were diluted with unlabeled guanine nucleotide prior to use, giving ~1000 disintegrations per min (dpm)/μM nucleotide.

Preparation of Ras Protein Samples. Human H-Ras-(1−166) and the Ras variant C118S(1−166) were expressed and purified as described previously (*38*, *39*). Matrix-assisted laser desorption/ionization time-of-flight mass spectrometry analysis was performed on Ras after purification. Results from this analysis indicated that the Cys^{118} thiol side chain of Ras exists in various oxidized states, typically consisting of the ~20−30% sulfhydryl (Ras Cys^{118}-H), ~10−30% sulfenic acid (Ras Cys^{118}-OH), ~30−40% sulfinate (Ras Cys^{118}-O_2^-), and ~10−20% sulfonate (Ras Cys^{118}-O_3^-). The proportion of the different oxidized states of the Ras Cys^{118} thiol side chain varies between samples and is likely to result from Ras Cys^{118} side-chain oxidation during purification under aerobic conditions. However, after incubation of the purified Ras protein with a reducing agent dithiothreitol (DTT, 10 mM) for 30 min under anaerobic conditions, most of Ras Cys^{118}-OH was reduced to Ras Cys^{118}-H. Hence, after Ras incubation with DTT, ~60% of Cys^{118} thiol side chain is present in the redox-active Ras Cys^{118}-H form. We also observed that reduction of Cys^{118}-OH to Ras Cys^{118}-H is more effective with DTT than either glutathione or cysteine, which is most likely due to the lower redox potential of DTT relative to that of glutathione and cysteine. The remaining fraction (i.e., ~30−40% Ras Cys^{118}-O_2^- and ~10−20% Ras Cys^{118}-O_3^-) can be reduced to Ras Cys^{118}-H by incubating with a strong reducing agent, titanium citrate, most likely because the redox potentials of sulfinyl and sulfonyl radicals are much higher than the biologically relevant ROS and RNS used in this study. However, treatment with titanium citrate can potentially reduce other redox-active residues such as histidine and threonine and thus may alter the Ras structure and/or activity. Therefore, for these studies, we employed DTT to treat the Ras samples, which resulted in ~60% of the sample existing in its redox-active Ras Cys^{118}-H state. The remaining ~40% exists in higher oxidized states, i.e., Ras Cys^{118}-O_2^- and Ras Cys^{118}-O_3^-, which renders this fraction of Ras redox-inactive under our experimental conditions. DTT was removed by passing Ras protein samples through a size-exclusion column (G-25, 1 × 5.0 cm) under anaerobic conditions. The column was pre-equilibrated anaerobically with metal-chelexed 5 mM ammonium acetate buffer (pH 7.5) containing 50 mM NaCl. Ras-SNO was produced and quantified by treatment of NO/O_2 as described previously (*18*, *19*). To label Ras or Ras-SNO with rhodamine, Ras or Ras-SNO (100 μM, 0.25 mL) was mixed with

rhodamine B (500 μM, 0.25 mL) in a buffer containing 20 mM GDP, 50 mM NaCl, 5 mM $MgCl_2$, and 100 μM diethylenetriaminepentaacetic acid (DPTA) in ammonium acetate (10 mM, pH 7.5) under anaerobic conditions and the mixture was incubated for 20 min at room temperature. The sample mixture was loaded onto a size-exclusion column (Sephadex G-25, 1.5 × 7 cm) at room temperature, pre-equilibrated anaerobically with the ammonium acetate buffer (10 mM, pH 7.5) containing 20 mM GDP, 50 mM NaCl, 5 mM $MgCl_2$, and 100 μM DPTA, to remove unreacted free rhodamine B from rhodamine-labeled Ras or Ras-SNO, and eluted at a rate of 0.5 mL/min. A fluorescence assay (*18*−*20*) was employed to assess the rate of guanine nucleotide dissociation from rhodamine-labeled Ras and Ras-SNO. Results from this assay indicate that rhodamine labeling does not affect the intrinsic rate of Ras guanine nucleotide dissociation. The Raf-RBD fragment (Raf-1 residues 50−131) was expressed as a GST fusion protein using a pGEX4T expression vector and purified by affinity separation on glutathione agarose beads. The GST affinity tag was cleaved with thrombin. All isolated proteins were >95% pure as determined by SDS−PAGE, and the protein concentration was determined by the Bradford method (*40*).

Generation and Quantification of Redox Agents. NO gas (Aldrich) was purified by passing it through a scrubbing column with 5 M KOH prior to use in experiments (*18*). The amount of NO used in the assay was quantified using a hemoglobin-coupled assay (*18*). $^{\cdot}NO_2$ was generated by the addition of O_2 into the NO-containing assay solution as previously described (*18*). XO (Sigma) was used to generate $O_2^{\cdot-}$ (*20*). A spectrophotometric assay using 4-chloro-7-nitrobenzo-2-oxa-1,3-diazole (Aldrich) was used for $O_2^{\cdot-}$ quantifications (*41*), and bovine liver Cu/Zn superoxide dismutase (SOD, Sigma) (*42*) was employed to scavenge $O_2^{\cdot-}$. H_2O_2 was treated with a mixture of transition metals (1 mM $CuCl_2$ and 1 mM $FeCl_2$) to produce the redox species, $O_2^{\cdot-}$ and $OH^{\cdot}$, following the Fenton reaction (*26*). Given that 4-chloro-7-nitrobenzo-2-oxa-1,3-diazole may also react with $OH^{\cdot}$, the exact content of $OH^{\cdot}$ and $O_2^{\cdot-}$ in the assay mixture was not determined. A stock solution of $ONOO^-$ (Alexis, San Diego, CA) was prepared by following the procedure specified by the factory protocol. The concentration of $ONOO^-$ was determined spectrophotometrically at 302 nm before use, using a molar absorption of $e_{302} = 1.67 \times 10^3$ M^{-1} cm^{-1}. However, the exact concentrations of $ONOO^-$ decomposition products (i.e., $^{\cdot}NO_2$ and $OH^{\cdot}$) were not determined.

Experimental Conditions. All assays and sample preparations were performed in serum-stoppered sealed cuvettes and vials to avoid diffusion of volatile redox agents (i.e., NO, $^{\cdot}NO_2$, $O_2^{\cdot-}$, H_2O_2, or $OH^{\cdot}$) into the open atmosphere. To prevent transition-metal-mediated conversion of the $O_2^{\cdot-}$ radical into H_2O_2 and $OH^{\cdot}$ (*28*) as well as NO into nitrosonium ion (NO^+) (*18*), all buffers used for kinetic and biochemical assays were passed through a metal-chelating Bio-Rad Chelex-100 cation-exchange column (*43*) and 100 μM DPTA was added to the buffers prior to performing the experiments, unless otherwise noted. When necessary, high-grade transition-metal-free $MgCl_2$ and NaCl (Aldrich) were added to the transition-metal-free buffer, and DPTA was omitted in the H_2O_2/transition-metal-mediated Ras guanine nucleotide dissociation kinetic assays and mass spectrometry (MS) sample preparations. Although the solution concentrations of NO can be directly estimated (*18*), the concentration of $O_2^{\cdot-}$ generated in the XO assay is not fixed during the $O_2^{\cdot-}$-mediated GTPase guanine nucleotide dissociation process, because XO can continuously produce $O_2^{\cdot-}$ with time (*20*). Moreover, we have found that the XO substrate, xanthine, and its enzymatic reaction product, uric acid, quench XO-produced $O_2^{\cdot-}$. To aid in quantification of $O_2^{\cdot-}$ in the assay, a minimal amount of XO was incubated in the assay solution for a given time t to accumulate $O_2^{\cdot-}$ prior to initiating the assay. The concentration of accumulated $O_2^{\cdot-}$ was then estimated spectrophotometrically using 4-chloro-7-nitrobenzo-2-oxa-1,3-diazole (*41*).

In principle, the rate of guanine nucleotide dissociation upon treatment of Ras with redox agents (i.e., $^{\cdot}NO_2$) can be monitored with either the fluorescence 2′-(or-3′)-*O*-(*N*-methylanthraniloyl)guanosine 5′-diphosphate (mant-GDP) or radiolabeled nucleotide (i.e., [^{3}H]GDP) kinetic assay (*20*). Because high-energy UV light (i.e., >260 nm) may promote cleavage of GSNO into $GS^{\cdot}$ and NO (*44*) and the fluorescence mant-GDP assay requires illumination at 365 nm to stimulate mant fluorescence (*45*), GSNO-mediated mant-GDP dissociation from Ras may result from the production of the photolytic GSNO cleavage product $GS^{\cdot}$, which can react with Ras-Cys^{118} thiol to produce Ras-$Cys^{118\cdot}$ and GS^- (*18*). The other photolytic cleavage product, NO, is unlikely to promote Ras guanine nucleotide dissociation, because the assay system did not contain O_2 necessary for the production of $^{\cdot}NO_2$ (*18*). Similarly, if Ras-SNO is illuminated at 365 nm, it is possible that some fraction of Ras-SNO may undergo cleavage to Ras-$Cys^{118\cdot}$ and NO. Moreover, we have observed that mant fluorescence is slightly quenched (~20%) in the presence of redox-active agents (i.e., $^{\cdot}NO_2$ and $O_2^{\cdot-}$). Hence, for kinetic assays with Ras-SNO, we employed a radioactivity assay to measure Ras GNE to eliminate the possibility of photolytic cleavage of Ras-SNO into Ras-$Cys^{118\cdot}$ and NO as well as fluorescence quenching of mant-GDP by redox agents in the solution. However, Ras Raf-1 RBD binding was measured using a fluorescence rhodamine-labeled Ras assay, because illumination of Ras-SNO at lower energy wavelengths (i.e., 490 nm) minimizes photolytic cleavage. Although rhodamine can react with a small fraction of the available redox agent(s), the fluorescence properties of rhodamine were not significantly altered.

Kinetic Measurements of Ras Guanine Nucleotide Exchange. A standard assay solution for the measurements consisted of transition-metal-free 50 mM NaCl, 5 mM $MgCl_2$, and 100 μM DPTA in ammonium acetate buffer (10 mM, pH 7.5) and was treated with redox agents (i.e., NO/O_2, $O_2^{\cdot-}$, H_2O_2/transition metals, or $ONOO^-$) prior to the addition of Ras or Ras-SNO. To measure the rates of NO/O_2-, $O_2^{\cdot-}$-, H_2O_2/transition metals-, or $ONOO^-$-mediated Ras or Ras-SNO GDP dissociation [$^{\cdot NO_2}k_{\text{off (Ras−GDP)}}$, $^{O_2^{\cdot-}}k_{\text{off (Ras−SNO−GDP)}}$, $^{H_2O_2/\text{metals}}k_{\text{off (Ras−GDP)}}$, or $^{ONOO^-}k_{\text{off (Ras−SNO−GDP)}}$, respectively], [^{3}H]GDP-preloaded Ras or [^{3}H]GDP-preloaded Ras-SNO was added to an assay mixture containing the redox agent in the presence of unlabeled GDP. To measure rates of NO/O_2- or H_2O_2/transition-metal-mediated Ras GTP association [$^{\cdot NO_2}k_{\text{on (Ras−GTP)}}$ or $^{H_2O_2/\text{metals}}k_{\text{on (Ras−GTP)}}$], unlabeled GDP-preloaded Ras was introduced into the standard assay solution containing an appropriate redox agent in the presence of free [^{3}H]GTP. In

some assays, the radical scavenger agent, ascorbate, was added to the assay mixture during the assay time period. The change in radioactivity of the Ras-bound nucleotide over time was determined using a Beckman−Coulter scintillation counter. Rates [i.e., $^{\cdot NO_2}k_{off\ (Ras-GDP)}$] were determined by fitting the data to a simple exponential decay and exponential association, respectively. The equilibrium dissociation constant for Ras GTP binding to Ras GDP in the presence of NO/O_2 (via $\cdot NO_2$, $^{\cdot NO_2}K_{D\ GDP/GTP}$) (eq 1) was determined from the ratio of $^{\cdot NO_2}k_{off\ (Ras-GDP)}$ and $^{\cdot NO_2}k_{on\ (Ras-GTP)}$

$$^{\cdot NO_2}K_{D\ GDP/GTP} = {}^{\cdot NO_2}k_{off\ (Ras-GDP)}/{}^{\cdot NO_2}k_{on\ (Ras-GTP)} \quad (1)$$

Similarly, the ratio of $^{\cdot NO_2}k_{off\ (Ras-GDP)}$ and $^{\cdot NO_2}k_{on\ (Ras-GDP)}$ was used to determine the equilibrium dissociation constant for Ras GDP with GDP ($^{\cdot NO_2}K_{D\ GDP/GDP}$) (eq 2)

$$^{\cdot NO_2}K_{D\ GDP/GDP} = {}^{\cdot NO_2}k_{off\ (Ras-GDP)}/{}^{\cdot NO_2}k_{on\ (Ras-GDP)} \quad (2)$$

Binding of the Raf-1 RBD to Either Ras or Ras-SNO in the Presence or Absence of $O_2^{\cdot -}$. Either rhodamine-labeled Ras or Ras-SNO was introduced into a GDP- or GTP-containing standard assay solution, and the Raf-1 RBD was added before and after the addition of XO to account for the intrinsic and $O_2^{\cdot -}$-mediated Ras binding to the Raf-1 RBD, respectively. The mixture was excited at 490 nm, and the fluorescence emission band at 500−650 nm was monitored using a LS50B Perkin−Elmer fluorimeter.

Mass Spectrometry Analysis. Nucleotide oxygenation or nitrosylation product(s) released from either Ras- or Ras-SNO upon treatment with H_2O_2/transition metals, $O_2^{\cdot -}$, or $ONOO^-$ in the presence and absence of CO_2 were separated from Ras using a centricon (10-kDa cut off, Millipore). An aliquot of the sample was dissolved in 50% methanol/0.1% formic acid, because sample acidification with formic acid allows MS detection of positively charged ions (i.e., $[M + H]^+$). Therefore, the molecular weights determined by MS are 1 Da higher (m/z) than the molecular weights for the same chemicals at neutral pH (i.e., pH 7.5). The acidified sample (~1 μL) was loaded into a Protana distal coated nanospray needle (Protana, Odense, Denmark), and spectra acquired over a mass range of 400−500 in MS mode using nanospray mass spectrometry on an ABI QSTAR-Pulsar QTOF MS spectrometer with a nanoelectrospray source (Applied Biosystems Division, Perkin−Elmer Corp., Foster City, CA).

RESULTS

H_2O_2/Transition-Metal- and Peroxynitrite-Mediated Ras Guanine Nucleotide Dissociation. We have previously shown that H_2O_2 (in the absence of transition metals) does not facilitate Ras guanine nucleotide dissociation *in vitro* (*20*). However, when a transition metal (Cu^{2+} or/and Fe^{2+}) is present under aerobic conditions at physiological pH (i.e., pH 7.5), H_2O_2 can be converted into $O_2^{\cdot -}$ and a small fraction of $OH^{\cdot}$ (*26*, *27*, *46*). Because cells contain various transition metals, the observed rate of Ras GNE by H_2O_2 in cells (*37*) may be an $O_2^{\cdot -}$- and/or $OH^{\cdot}$-mediated radical-based process. To examine whether H_2O_2/transition-metal-derived $O_2^{\cdot -}$ and/or $OH^{\cdot}$ facilitates Ras guanine nucleotide dissociation, we conducted Ras guanine nucleotide dissociation assays in the presence of H_2O_2 and the transition metals, Cu^{2+} and/or Fe^{2+} (Figure 1A). Consistent with our previous results (*20*), H_2O_2 itself (in the absence of transition metals) does not facilitate Ras guanine nucleotide dissociation, yet when the transition metals were added to the assay system (thus, $O_2^{\cdot -}$ and $OH^{\cdot}$ are formed), Ras guanine nucleotide dissociation was observed (Figure 1A), with a rate of H_2O_2/transition-metal-mediated Ras guanine nucleotide dissociation ($^{H_2O_2/metals}k_{off\ (Ras-GDP)} = 2.9 \times 10^{-3}\ s^{-1}$) similar to that of NO/O_2- or $O_2^{\cdot -}$-mediated Ras guanine nucleotide dissociation (*18*−*20*). To aid in the identification of redox-active species generated in the H_2O_2/transition-metal-containing assay mixture used for Ras guanine nucleotide dissociation, SOD, an $O_2^{\cdot -}$ scavenger, was added to the assay system. As shown in Figure 1A, both the rate and span of H_2O_2/transition-metal-mediated Ras guanine nucleotide dissociation are drastically decreased in the presence of SOD, indicating that $O_2^{\cdot -}$ is the active reactive radical species that facilitates Ras guanine nucleotide dissociation. However, SOD does not completely block H_2O_2/transtion-metal-mediated Ras guanine nucleotide dissociation, suggesting that $OH^{\cdot}$, in addition to $O_2^{\cdot -}$, may also serve as an active radical species in the H_2O_2/transition-metal-containing assay mixture. Intriguingly, the slow rate and reduced span of H_2O_2/transtion-metal-mediated Ras C118S guanine nucleotide dissociation in the presence of SOD is similar to that of the H_2O_2/transtion-metal-mediated Ras guanine nucleotide dissociation in the presence of SOD (Figure 1A). The Ras C118S variant possesses a serine instead of the redox-active cysteine at position 118 of Ras, and we have previously shown that neither $O_2^{\cdot -}$ nor NO/O_2 (via $\cdot NO_2$) promote guanine nucleotide dissociation on this variant (*18*−*20*). However, because a small enhancement in H_2O_2/transition-metal-mediated Ras guanine nucleotide dissociation is observed for Ras C118S in the presence and absence of SOD, we speculate that the serine residue of Ras C118S may react with $OH^{\cdot}$ to produce a Ras C118S serine radical (Ras C118S−$O^{\cdot}$) and, subsequently, Ras C118S−$O^{\cdot}$ may facilitate Ras guanine nucleotide dissociation by a mechanism similar to that of $\cdot NO_2$- and $O_2^{\cdot -}$-mediated Ras guanine nucleotide dissociation (*18*−*20*). Although these kinetic results suggest that $O_2^{\cdot -}$ is the primary active radical species produced in the H_2O_2/transition-metal mixture that facilitates Ras guanine nucleotide dissociation, $OH^{\cdot}$ may also contribute to Ras guanine nucleotide dissociation under our experimental conditions.

As shown in Figure 1B, $ONOO^-$ also facilitates Ras guanine nucleotide dissociation, with the rate of $ONOO^-$-mediated Ras guanine nucleotide dissociation similar to that of NO/O_2-, $O_2^{\cdot -}$-, and H_2O_2/transition-metal-mediated Ras guanine nucleotide dissociation. Given that $ONOO^-$ can be decomposed into $\cdot NO_2$ and a small fraction of $OH^{\cdot}$ (*23*), the observed $ONOO^-$-mediated rate of Ras guanine nucleotide dissociation may be mediated by both $\cdot NO_2$ and $OH^{\cdot}$ in the reaction mixture. It is possible that $OH^{\cdot}$, if present, in the assay mixture, could produce $O_2^{\cdot -}$ via the reaction with O_2 and thus contribute to the rate of Ras guanine nucleotide dissociation (*58*). However, because $ONOO^-$-mediated Ras guanine nucleotide dissociation (Figure 1B) is not inhibited by SOD treatment, it is unlikely that $OH^{\cdot}$ contributes significantly to Ras GNE. These results indicate that the observed rate of $ONOO^-$-mediated Ras guanine nucleotide

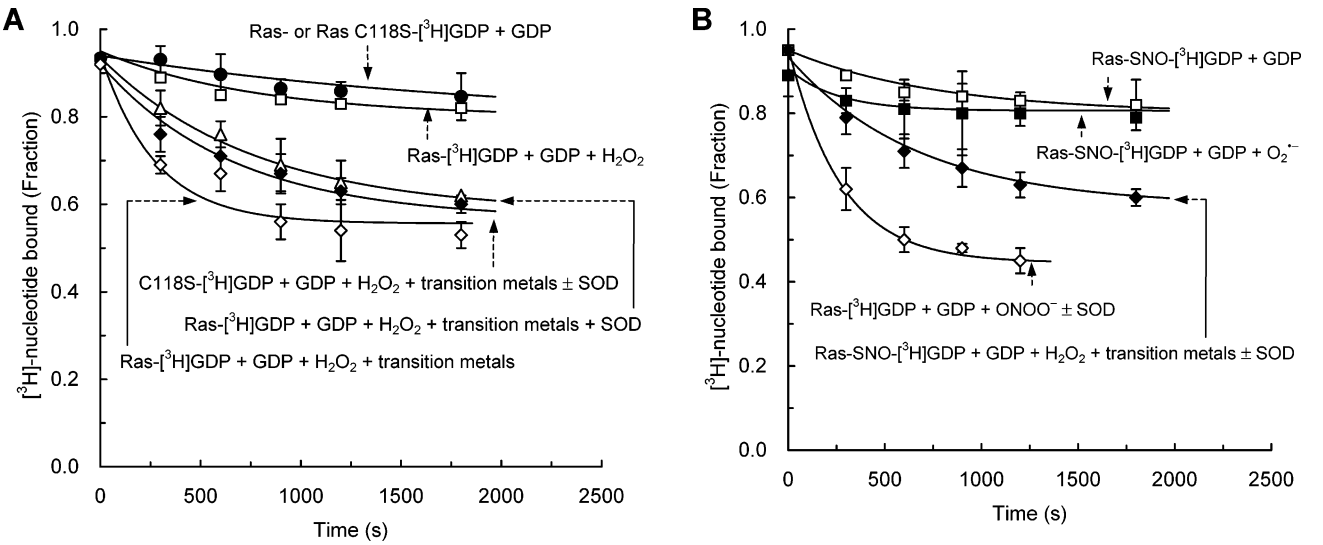

FIGURE 1: Determination of H_2O_2/transition-metal- and SIN-1-mediated Ras and Ras-SNO GDP dissociation rates. H_2O_2 (0.01%, v/v) in the absence and presence of a mixture of transition metals $CuCl_2$ (0.1 mM) and $FeCl_2$ (0.1 mM) or $ONOO^-$ (10 μM) was incubated for 5 min prior to the addition of [^{3}H]GDP-loaded Ras (1 μM). XO (unit activity = 5.0 μM s^{-1}) was incubated with its substrate xanthine (5 mM) for 30 min to accumulate $O_2^{\cdot-}$ in solution prior to the addition of [^{3}H]GDP-loaded Ras (1 μM). When indicated, SOD (~1000 units) was added to the redox-containing assay solution and incubated for 10 min prior to the addition to the GTPase. For these assays, assay vials were sealed to prevent the diffusion of treated redox agents (H_2O_2, H_2O_2/transition metals, $O_2^{\cdot-}$, and $ONOO^-$) into the open atmosphere. As a control, the intrinsic GDP dissociation rates of Ras, Ras-SNO, and Ras C118S were also measured using experimental conditions identical to those described above, except that the redox agent was not added. For all assays, aliquots were withdrawn at specific time points and spotted onto nitrocellulose filters. The filters were then washed 3 times with an assay buffer, and radioactivity was determined using Beckman−Coulter scintillation counter. The resultant radioactivity (dpm values) associated with Ras-bound [^{3}H]GDP was converted into the fraction of moles of nucleotide per moles of total Ras. Rates of intrinsic and redox-mediated GDP dissociation were obtained by fitting the data to a simple exponential decay. The intrinsic Ras, Ras-SNO, and Ras C118S GDP dissociation rates were determined to be 0.02×10^{-3}, 0.11×10^{-3}, and 0.02×10^{-3} s^{-1}, respectively. The H_2O_2- and H_2O_2/transition-metal-mediated Ras GDP dissociation rates were determined to be 0.08×10^{-3} and 2.94×10^{-3} s^{-1}, respectively, and the rates of H_2O_2/transition-metal-mediated Ras-SNO GDP dissociation in the presence and absence of SOD were determined to be 0.15×10^{-3} and 2.06×10^{-3} s^{-1}, respectively. The rates of H_2O_2/transition-metal-mediated Ras C118S GDP dissociation in the presence and absence of SOD were determined to be the same, 0.13×10^{-3} s^{-1}. The Ras-SNO GDP dissociation rates in the presence of $O_2^{\cdot-}$ and $ONOO^-$ were determined to be 0.12×10^{-3} and 2.88×10^{-3} s^{-1}, respectively. Figure symbol "+" represents the "presence of a chemical", e.g., GDP and/or a redox agent. Figure symbol "± SOD" designates the "presence or absence of SOD". The data presented in the figure represent mean values of triplicate measurements. Standard errors of each data point are <34%, and the regression values associated with the fit, r^2, were <0.7555.

dissociation is primarily driven by $ONOO^-$-derived $^{\cdot}NO_2$ in the reaction mixture.

In addition, $ONOO^-$ can immediately react with CO_2 to produce $CO_3^{\cdot-}$ and $^{\cdot}NO_2$ stoichiometrically 1:1 (*25*). Because of the relatively high redox potential of $CO_3^{\cdot-}$ (E_7 = ~1.8 V versus NHE) (*21*) compared to that of NO_2 and $O_2^{\cdot-}$ (*21*, *24*), $CO_3^{\cdot-}$ could react with the Ras Cys^{118} thiol to generate Ras-$S^{118\cdot}$ and facilitate Ras guanine nucleotide dissociation. To examine the effects of $CO_3^{\cdot-}$ on Ras guanine nucleotide dissociation, the $^{\cdot}NO_2$-selective scavenger, reduced hemoglobin (100 μM) was added into the reaction mixture of $ONOO^-$ and CO_2. A significantly reduced rate and span of $ONOO^-/CO_2$-mediated Ras guanine nucleotide dissociation was observed (not shown), suggesting that both $CO_3^{\cdot-}$ and $^{\cdot}NO_2$ formed by the addition of CO_2 to $ONOO^-$ facilitate Ras guanine nucleotide dissociation.

Detection and Characterization of Nucleotide End Products Released from Ras upon Exposure to H_2O_2 in the Presence of Transition Metals and Peroxynitrite. Our kinetic results indicate that $O_2^{\cdot-}$ is the primary redox-active agent in the H_2O_2/transition-metal-assay mixture, which promotes Ras guanine nucleotide dissociation. If this is indeed the case, Ras-$Cys^{118\cdot}$ generated from the reaction of the Ras Cys^{118} thiol with $O_2^{\cdot-}$ and $OH^{\cdot}$ is expected to undergo radical propagation to Ras-bound GDP via the Phe^{28} side chain to produce Ras-bound $G^{\cdot}$-DP. Ras-bound $G^{\cdot}$-DP can then react with another $O_2^{\cdot-}$ and/or $OH^{\cdot}$ to produce the oxygenated-GDP adducts, 5-oxo-GDP (*20*, *47*) and 5-hydroxy-GDP (Figure 2), respectively. We have previously characterized the degradation products of 5-oxo-GDP formed by the reaction of Ras-bound $G^{\cdot}$-DP with $O_2^{\cdot-}$ (*20*, *47*). 5-Diamino-4*O*-imidazolone ribose diphosphate (DIm-DP) is formed after decarboxylation of 5-oxo-GDP, which can be further degraded into 5-amino-4*O*-imidazolone ribose diphosphate (AIm-DP; MW = 415.26 Da), 5-imino-4*O*-imidazolone ribose diphosphate (IIm-DP; MW = 417.26 Da), and/or 5-diamino-4*O*-2-methyl-imidazolone ribose diphosphate (DMm-DP; MW = 465.26 Da). Similar to 5-oxo-GDP, 5-hydroxy-GDP is unstable and, as shown in Figure 2, can be degraded into various oxygenated-GDP derivatives. 5-Amino-4-hydroxy-imidazolone ribose diphosphate [1-(4-hydroxy-1*H*-imidazole-5-yl)guanidinum ribose diphosphate, HIm-DP; MW = 420.19 Da] can be formed after decarboxylation of 5-hydroxy-GDP (step iv in Figure 2). It is noteworthy that the oxygenated-GDP degradation products derived from the treatment of Ras with H_2O_2/transition metals are dependent upon the experimental conditions (i.e., amount of methanol, ethanol, or acid in the sample preparation mixture), yet to conveniently identify the degradation forms of 5-oxo-GDP, we have employed nearly identical experimental conditions to those used previously (*20*, *47*). MS analyses of guanine nucleotide adducts released from Ras

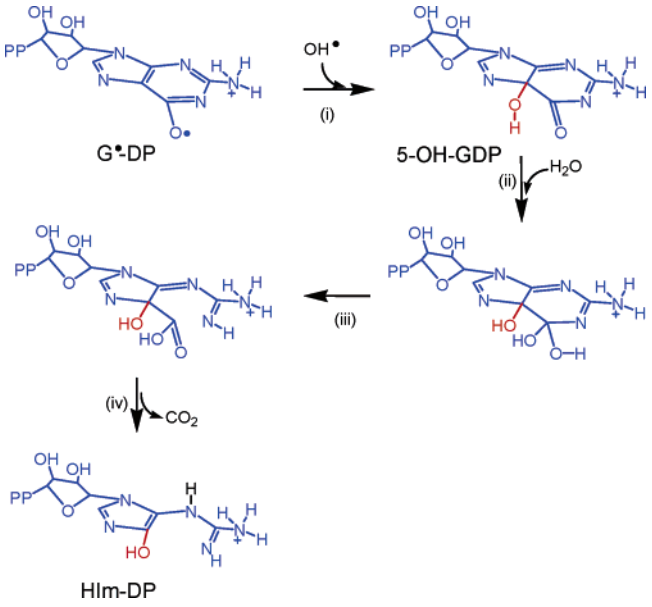

FIGURE 2: Proposed guanine nucleotide degradation products upon exposure of Ras to H_2O_2/transition metals. GDP and the GDP-oxygenated adducts are represented in blue and red, respectively.

upon exposure to H_2O_2/transition metals are shown in Figure 3A. MS peaks are observed at 415.26, 417.26, 465.26, as well as 420.19 that correspond to the molecular weight of the 5-oxo-GDP derivatives, AIm-DP, IIm-DP, DMm-DP, as well as the 5-hydroxy-GDP derivative, HIm-DP, respectively. These data provide support that $O_2^{\cdot-}$ as well as $OH^{\cdot}$ are indeed present in the H_2O_2/transition-metal-containing assay solution and can react with Ras-bound G$^{\cdot}$-DP to produce 5-oxo-GDP and 5-hydroxy-GDP, respectively. The molecular structures and chemical properties (i.e., charges) of these oxygenated-GDP derivatives are similar. Hence, the MS peak intensities associated with these oxygenated-GDP derivatives are comparable. Because the MS peak intensity for the 5-oxo-GDP derivative (i.e., DMm-DP) is larger than that of the 5-hydroxy-GDP derivative (HIm-DP), $O_2^{\cdot-}$ may be the dominant reaction species in the H_2O_2/transition-metal-containing assay solution to react with G$^{\cdot}$-DP to produce 5-oxo-GDP. Formation of 5-oxo-GDP derivatives, AIm-DP, IIm-DP, and DMm-DP, in XO-generated $O_2^{\cdot-}$-mediated Ras guanine nucleotide dissociation is also shown for a comparison (Figure 3B) (*20*, *47*). Although the primary MS peaks corresponding to the degradation products derived from H_2O_2/transition-metal-mediated Ras guanine nucleotide dissociation can be assigned, minor multiple unassigned MS peaks were also observed (Figure 3A). $OH^{\cdot}$ possesses a high redox potential (*21*); thus, it not only reacts with O_2 to produce $O_2^{\cdot-}$, but it can also react with various chemicals in the assay mixture to produce other forms of reactive radicals, which may then react with Ras-bound G$^{\cdot}$-DP to produce these minor MS peaks. Further studies are required to assign the unidentified minor MS peaks.

Our kinetic results suggest that $ONOO^-$ primarily decomposes to $^{\cdot}NO_2$, which can then react with the Ras-Cys^{118} thiol to produce Ras-Cys$^{118\cdot}$, resulting in an enhanced rate of Ras nucleotide dissociation. Several assigned and unidentified MS peaks were detected from Ras exposed to $ONOO^-$ (Figure 3C). The main MS peak was identified to be 5-guanidino-4-nitroimidazole ribose diphosphate, NIm-DP; MW = 463.32 Da) (*19*), a nitrated-GDP (5-nitro-GDP) degradation product. Minor MS peaks derived from 5-oxo-GDP and 5-hydroxy-GDP were also observed, as well as some unidentified peaks. The unidentified MS peaks may be derived from the reaction of Ras-bound G$^{\cdot}$-DP with uncharacterized reactive radical species derived from $ONOO^-$. Nevertheless, our data indicate that a Ras sample-treated with $ONOO^-$ contains at least three reactive radical species based on MS peaks assignments: (i) primarily $^{\cdot}NO_2$, (ii) a small fraction of $O_2^{\cdot-}$, and (iii) trace amounts of $OH^{\cdot}$. All of three of these redox-active species can react with bound G$^{\cdot}$-DP to produce various GDP radical adducts: 5-nitro-GDP, 5-oxo-GDP, and 5-hydroxy-GDP. Similar to the H_2O_2/transition-metal-containing assay mixture, $OH^{\cdot}$, derived from $ONOO^-$, may lead to the generation of $O_2^{\cdot-}$ because of the reaction with O_2. If Ras guanine nucleotide dissociation is coupled with $ONOO^-$, the nitrated- and oxygenated-GDP derivatives cannot be formed, because a direct (two-electron) nucleophilic reaction with the Ras-Cys^{118} thiol to produce a Ras-ONOO adduct (Ras-Cys^{118}—O_2NO) is not a radical reaction process. These results therefore suggest that $ONOO^-$ promotes Ras guanine nucleotide dissociation primarily through a $^{\cdot}NO_2$ radical-based process, consistent with our kinetic results. However, other $ONOO^-$ degradation products, $O_2^{\cdot-}$ and $OH^{\cdot}$, may also contribute to a minor extent. When Ras was treated with a mixture of $ONOO^-$ and CO_2, a few additional MS peaks were detected, in addition to the 5-nitro-GDP degradation product peak (Figure 3D). We are unable to assign all of the additional MS peaks. However, 5-guanidino-4-carbonate-imidazole ribose diphosphate ([1-(4-carbonate-1*H*-imidazole-5-yl)guanidine ribose diphosphate], CIm-DP; MW = 477.32 Da) was assigned as a carbonated-GDP degradation product. These results and analyses suggest that $CO_3^{\cdot-}$, in addition to $^{\cdot}NO_2$, is present in the mixture containing both $ONOO^-$ and CO_2 and reacts with bound G$^{\cdot}$-DP to produce a carbonated-GDP adduct.

Effects of Redox Agents on S-Nitrosylated Ras. We have previously postulated that S-nitrosylated Ras (Ras-SNO) can be formed by a series of reactions of the Ras-Cys^{118} thiol with $^{\cdot}NO_2$ and NO (*19*), in that the initial reaction of $^{\cdot}NO_2$ with Ras-Cys^{118} produces Ras-Cys$^{118\cdot}$, which then facilitates the dissociation of Ras-bound GDP as 5-nitro-GDP and an apo Ras Cys^{118} thiolate (Ras-Cys^{118-}). The second reaction of $^{\cdot}NO_2$ with Ras-Cys^{118-} may then produce apo Ras-Cys$^{118\cdot}$. However, at this stage, the Ras-bound GDP electron donor is not available for electron transfer to apo Ras-Cys$^{118\cdot}$, because GDP has been released from Ras as 5-nitro-GDP. Thus, if both NO and guanine nucleotide (i.e., GTP) are present at this stage, apo Ras-Cys$^{118\cdot}$ should be able to react with NO to produce apo Ras-SNO, which then rebinds the available guanine nucleotide to produce GTP-bound Ras-SNO (*18*, *19*). Consistent with this premise, subsequent addition of NO followed by NO/O_2 ($^{\cdot}NO_2$) as a radical quencher generates active GTP-bound Ras-SNO (not shown). However, given that treatment of Ras-SNO with a NO/O_2 reaction mixture (containing $^{\cdot}NO_2$) is unable to facilitate guanine nucleotide dissociation from Ras-SNO (*19*), the sulfur atom in the Ras SNO moiety may not react with $^{\cdot}NO_2$. Accounting for these results, we anticipate that $O_2^{\cdot-}$ will not enhance guanine nucleotide dissociation from Ras-SNO because it possesses a similar redox potential to $^{\cdot}NO_2$ (*21*, *24*). In agreement with this premise, we show that $O_2^{\cdot-}$ does not facilitate GDP dissociation of Ras-SNO (Figure 1B).

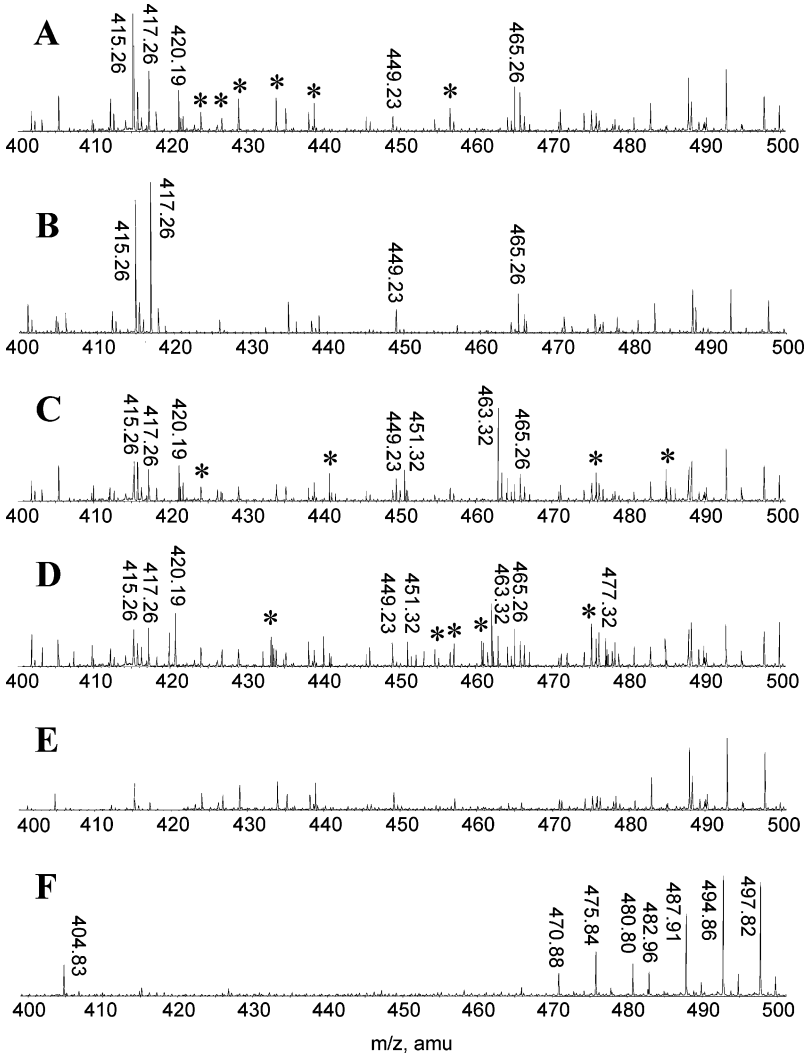

FIGURE 3: Molecular-weight determination of guanine nucleotide adducts released from Ras upon treatment with H_2O_2/transition metals and peroxynitrite in the presence and absence of CO_2 by MS. (A) H_2O_2 (0.01%) and a transition-metal mixture containing $CuCl_2$ (0.1 mM) and $FeCl_2$ (0.1 mM) were added to the assay buffer and incubated for 5 min (final volume of 900 μL) in a sealed vial. GDP-loaded Ras (1 μM, 100 μL) was then added to the H_2O_2/transition-metal-containing assay mixture and incubated for 10 min. (B) $O_2^{\cdot-}$ was produced by the addition of XO (activity = 0.4 μM^{-1} s^{-1}) and xanthine (10 mM) in the assay solution (final volume of 900 μL). XO and xanthine were incubated for 30 min in a sealed vial prior to the addition of GDP-loaded Ras (1 μM, 100 μL). The sample mixture was then incubated for 10 min. (C) Authentic $ONOO^-$ (10 μM) was introduced into a sealed vial containing the assay solution (final volume of 900 μL) and was incubated for 5 min prior to the addition of GDP-loaded Ras (1 μM, 100 μL). The sample mixture was then incubated for 10 min. (D) $ONOO^-$ (10 μM) and CO_2 (10 μM) were introduced into a sealed vial containing the assay solution (final volume of 900 μL) and were incubated for 5 min prior to the addition of GDP-loaded Ras (1 μM, 100 μL). The sample mixture was then incubated for 10 min. (E) $O_2^{\cdot-}$ was produced by the addition of XO (activity = 0.4 μM^{-1} s^{-1}) and xanthine (10 mM) in the assay solution (final volume of 900 μL) in a sealed vial and incubated for 30 min prior to the addition of GDP-loaded Ras-SNO (1 μM, 100 μL). The sample mixture was incubated for 10 min. (F) For a control, GDP-loaded Ras was added to the assay solution in the absence of H_2O_2/transition metals, XO, and $ONOO^-$. Fractions containing the nucleotide products from the samples A−E as well as the control F were prepared and analyzed by MS as described in the Experimental Procedures. For each assigned chemical adduct, two additional satellite peaks can be observed because of the presence of isomers of the assigned chemical adducts (*19*, *20*). Unassigned minor peaks are noted as "∗".

Moreover, when Ras-SNO was treated with $O_2^{\cdot-}$, neither 5-oxo- nor 5-hydroxy-GDP derivatives were detected (Figure 3E). However, a moderate guanine nucleotide dissociation rate was observed upon the treatment of Ras-SNO with the H_2O_2/transition-metal-containing assay buffer (Figure 1B), which may result from a small amount of $OH^{\cdot}$ in the assay solution. We therefore postulate that the redox potential of $OH^{\cdot}$ (*21*), formed from transition-metal catalysis of H_2O_2, is higher than that of a Ras-SNO radical(s) (putatively either Ras-S$^{\cdot}$NO or/and Ras-SNO$^{\cdot}$), so that the reaction of $OH^{\cdot}$ with Ras-SNO produces a radical form of Ras-SNO, which then initiates radical-based Ras guanine nucleotide dissociation from Ras-SNO.

These results in conjunction with our previous study (*19*) indicate that the sulfur (or oxygen) atom of the Ras-SNO moiety can react with $OH^{\cdot}$ but not $^{\cdot}NO_2$ or $O_2^{\cdot-}$ to produce a Ras-SNO radical, suggesting that the formation of Ras-SNO may render Ras less reactive to either $^{\cdot}NO_2$ or $O_2^{\cdot-}$ but not $OH^{\cdot}$.

Kinetics of $^{\cdot}NO_2$-, $O_2^{\cdot-}$-, or H_2O_2/Transition-Metal-Mediated Ras GNE and Ras Activation. We have previously shown that both $^{\cdot}NO_2$ and $O_2^{\cdot-}$ facilitate Ras GNE in the presence of the radical-quenching agent ascorbate or NO (*18*−*20*). However, an enhancement in the rate of guanine nucleotide dissociation but not guanine nucleotide association can be observed in the absence of a radical-quenching agent.

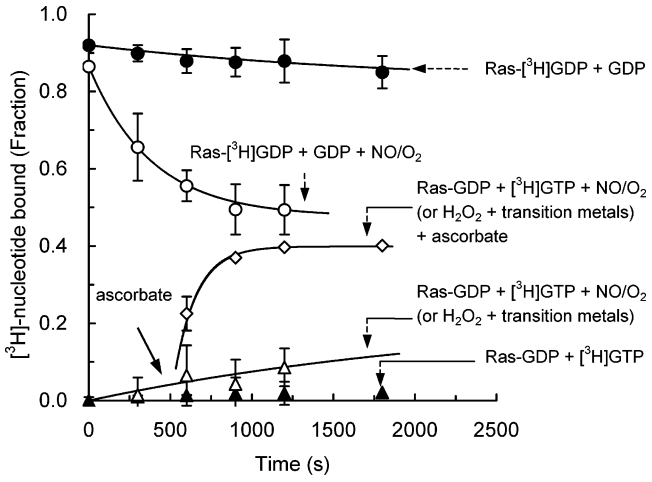

FIGURE 4: Determination of NO/O_2-mediated Ras GDP dissociation and GTP association rates. To monitor Ras GDP dissociation, [^{3}H]-GDP-loaded Ras (1 μM) and 20 mM GDP were added to the assay solution followed by the addition of either the NO/O_2 mixture ($\sim$5 μM NO and $\sim$10 μM O_2) or H_2O_2 (0.01%) in the presence of $CuCl_2$ (0.1 mM) and $FeCl_2$ (0.1 mM). To monitor Ras GTP dissociation, unlabeled-GDP-loaded Ras (1 μM) and 20 mM [^{3}H]GDP were added simultaneously to the assay solution followed by the addition of the NO/O_2 mixture ($\sim$5 μM NO and $\sim$10 μM O_2) or H_2O_2 (0.01%) in the presence of $CuCl_2$ (0.1 mM) and $FeCl_2$ (0.1 mM). The radical quenching agent, ascorbate (1 mM) or NO ($\sim$5 μM NO), was added to the assay mixture at an assay time of 500 s (indicated by an arrow). As controls, the intrinsic rates of Ras GDP dissociation and GTP association were also measured using experimental conditions identical to those described above, except that the redox agent was not added. Radioactivity assays were performed as described in Figure 1. The resultant radioactivity (dpm values) associated with Ras-bound radiolabeled nucleotide was converted into the fraction of moles of nucleotide per moles of total Ras. The intrinsic Ras GDP dissociation and GTP association rates were determined to be 0.02×10^{-3} s^{-1} and 0.06 M^{-1} s^{-1}, respectively. The Ras GDP dissociation rate in the presence of NO/O_2 was determined to be 2.73×10^{-3} s^{-1}. The rates of NO/O_2- and H_2O_2/transition-metal-mediated Ras GTP association in the absence and presence of ascorbate were determined to be 0.74 and 162.80 M^{-1} s^{-1}, respectively. The figure caption symbol "+" represents the "presence of a chemical", e.g., GDP and/or a redox agent. Rates of intrinsic and redox-mediated GDP dissociation were obtained by fitting the data to a simple exponential decay. The data presented in the figure are mean values of triplicate measurements. Standard errors of each data point are <43%, and the regression values associated with the fit were $r^2 < 0.7595$.

Thus, NO/O_2 (via $^{\cdot}NO_2$) and $O_2^{\cdot-}$ may promote GNE to form GTP-bound Ras in the presence of a radical-quenching agent under intracellular conditions, where GTP is in excess over GDP (*1*, *2*). Because the mechanism of H_2O_2/transition-metal-mediated Ras guanine nucleotide dissociation (this study) appears similar to that of $^{\cdot}NO_2$- and $O_2^{\cdot-}$-mediated Ras guanine nucleotide dissociation (*19*, *20*), we anticipate that treatment of Ras with H_2O_2/transition metals followed by ascorbate will facilitate Ras GDP exchange with GTP.

The second-order NO/O_2-mediated Ras GTP and GDP association rates, $^{\cdot NO_2}k_{on\ (Ras-GTP)}$ [$\sim$0.7 M^{-1} s^{-1} (Figure 4)] and $^{\cdot NO_2}k_{on\ (Ras-GDP)}$ [$\sim$0.6 M^{-1} s^{-1} (data not shown)], respectively, were estimated and used to assess the equilibrium dissociation constant for Ras GDP GNE with GTP in the presence of NO/O_2 ($^{\cdot NO_2}K_{D\ GDP/GTP}$ = $\sim$3.8 mM) following eq 1. The equilibrium dissociation constant ($^{ONOO^-}K_{D\ GDP/GTP}$ = $\sim$3.9 mM) in the presence of $ONOO^-$ instead of NO/O_2 (not shown) was also determined using an identical method. The Ras GDP dissociation constant with GDP in the presence of NO/O_2 ($^{\cdot NO_2}K_{D\ GDP/GDP}$) was also estimated and found to be 4.6 mM, using the estimated values of $^{\cdot NO_2}k_{off\ (Ras-GDP)}$ and $^{\cdot NO_2}k_{on\ (Ras-GDP)}$ for wt Ras in conjunction with eq 2. The somewhat higher $^{\cdot NO_2}k_{on\ (Ras-GTP)}$ and $^{\cdot NO_2}K_{D\ GDP/GTP}$ values compared to that of $^{\cdot NO_2}k_{on\ (Ras-GDP)}$ and $^{O_2^{\cdot-}}K_{D\ GDP/GDP}$ values could result from the slightly higher binding affinity of Ras for GTP relative to GDP (*45*). Although the equilibrium dissociation constant for Ras GDP GNE with GTP upon treatment with $O_2^{\cdot-}$ ($^{O_2^{\cdot-}}K_{D\ GDP/GTP}$) was not determined, the equilibrium dissociation constant for Ras GDP exchange with GDP in the presence of $O_2^{\cdot-}$ ($^{O_2^{\cdot-}}K_{D\ GDP/GDP}$ = 6.7 mM) was determined using the fluorescence method (*20*) and found to be similar to the value of $^{\cdot NO_2}K_{D\ GDP/GDP}$ (4.6 mM) shown in this study. Notably, the second-order rate of H_2O_2/transition-metal-mediated Ras GTP association rate ($^{H_2O_2/metals}k_{on\ (Ras-GTP)}$) and the equilibrium dissociation constant for Ras GDP GNE with GTP in the presence of H_2O_2/transition metals ($^{H_2O_2/metals}K_{D\ GDP/GTP}$) are similar to $^{\cdot NO_2}k_{on\ (Ras-GDP)}$ and $^{\cdot NO_2}K_{D\ GDP/GTP}$ (Figure 4). Given the large values of $^{\cdot NO_2}K_{D\ GDP/GTP}$, $^{\cdot NO_2}K_{D\ GDP/GDP}$, $^{ONOO^-}K_{D\ GDP/GTP}$, $^{O_2^{\cdot-}}K_{D\ GDP/GDP}$, and $^{H_2O_2/metals}K_{D\ GDP/GTP}$ and our data indicating that $^{\cdot}NO_2$ and $O_2^{\cdot-}$ are the primary redox-active species in the $ONOO^-$- and H_2O_2/transition-metal-containing assay mixtures, respectively, it is reasonable to suggest that $^{\cdot}NO_2$ and $O_2^{\cdot-}$ facilitate Ras guanine nucleotide dissociation but not Ras guanine nucleotide association, consistent with our previous results (*19*, *20*).

When the radical-quencher ascorbate (or NO) was added to NO/O_2- and H_2O_2/transition-metal-treated Ras and Ras GTP association measured (as indicated in an arrow in Figure 4), $^{\cdot NO_2}k_{on\ (Ras-GTP)}$ and $^{H_2O_2/metals}k_{on\ (Ras-GTP)}$ are greatly enhanced (estimated to be $\sim$160 M^{-1} s^{-1}), consistent with our previous study showing enhanced GDP reassociation of NO/O_2- or $O_2^{\cdot-}$-treated Ras in the presence of ascorbate or GSH (*19*, *20*). Similar kinetic values were obtained from measurements of $O_2^{\cdot-}$- and $ONOO^-$-mediated Ras GTP association (not shown). As stated earlier, if NO serves as a radical-quenching agent in the presence of GTP, GTP loading onto Ras-SNO can be observed, yet this form of Ras, Ras-SNO, does not further react with either $^{\cdot}NO_2$ or $O_2^{\cdot-}$, unless the NO moiety of Ras-SNO is removed.

When these results are taken together, they suggest that a radical quencher (i.e., ascorbate or NO) is required to facilitate Ras GDP GNE with GTP effectively by NO/O_2 (via $^{\cdot}NO_2$), H_2O_2/transition metals (mainly via $O_2^{\cdot-}$), $ONOO^-$ (mainly via $^{\cdot}NO_2$), or $O_2^{\cdot-}$, in agreement with our previous results (*19*, *20*).

Effect of $O_2^{\cdot-}$ on Ras GNE and Raf-RBD-Binding Interactions. Results described in Figure 4 indicate that the exchange of Ras GDP with GTP is facilitated by NO/O_2 or $O_2^{\cdot-}$ in the presence of a radical quencher to populate Ras in its active GTP-bound form. Given these results, we anticipate that Ras treated with either NO/O_2 or $O_2^{\cdot-}$ should enhance GTP-dependent binding interactions with downstream targets of Ras. To examine this hypothesis, we employed a fluorescence-based assay using rhodamine-labeled Ras and the Raf-1 RBD (*48*). When GDP-bound rhodamine-labeled Ras was titrated with the RBD of Raf-1, no increase in Ras-bound rhodamine fluorescence emission was observed (Figure 5A), indicating that GDP-bound Ras does not bind RBD with appreciable affinity over the RBD concentration range used in this study, in agreement with previous results

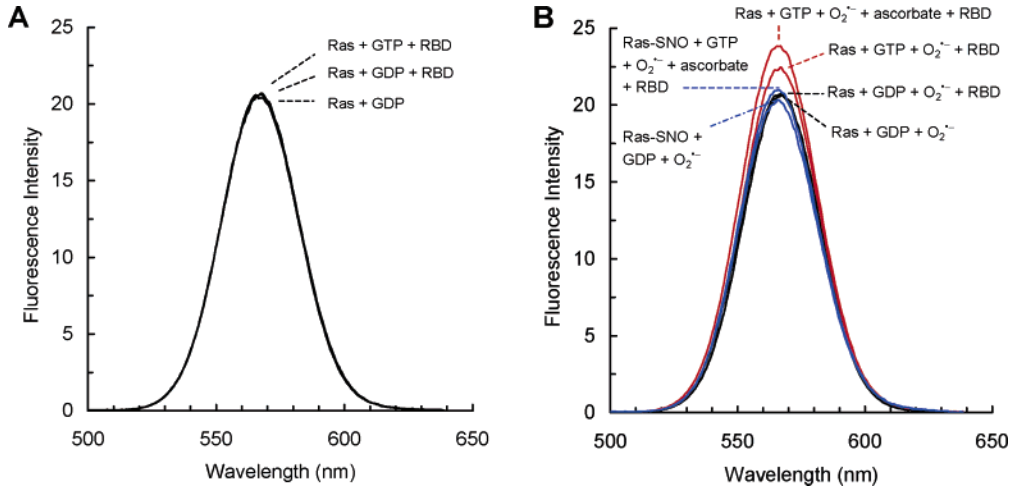

FIGURE 5: Effect of $O_2^{\cdot-}$ on Ras binding to the Raf-RBD. The standard assay buffer was employed for the Ras RBD binding assay and XO (activity = 5.2 μM^{-1} s^{-1}) was employed to produce $O_2^{\cdot-}$ as described previously (*20*). However, the XO substrate, xanthine (10 mM), was added prior to conducting the experiments. (A) Rhodamine-labeled GDP-bound Ras (2 μM) was incubated with GDP (20 mM) or GTP (20 mM) for 30 min in the absence of $O_2^{\cdot-}$ (without the treatment of XO) prior to the addition of the Raf-1 RBD (2 μM). (B) Rhodamine-labeled GDP-bound Ras (2 μM) or rhodamine-labeled GDP-bound Ras-SNO (2 μM) was treated with $O_2^{\cdot-}$ (by adding XO) for 30 min in the absence and presence of GDP (20 mM) or GTP (20 mM) prior to the addition of the Raf-1 RBD (2 μM). To examine the effect of a spin-trapping agent, ascorbate, on $O_2^{\cdot-}$-enhanced Ras Raf-RBD binding in the presence of GTP, ascorbate (1 mM) was added followed by the addition of the Raf-1 RBD (2 μM). Rhodamine-labeled Ras and Ras-SNO was excited at 490 nm, and the fluorescence emission band at 500−650 nm was monitored. The maximum fluorescence emission from rhodamine-labeled Ras and Ras-SNO was determined to be 547 and 546 nm, respectively. A slight blue shift (~1 nm) was observed in the Ras-SNO rhodamine fluorescence emission spectrum compared to that of Ras, which may be due to a slight interference associated with the SNO moiety energy transition (542 nm) (*18*). The Ras and Ras-SNO rhodamine fluorescence emission spectra in the presence of GTP, $O_2^{\cdot-}$, and/or RBD are shown in red and blue, respectively. The control Ras rhodamine fluorescence emission spectra in the presence of GDP, $O_2^{\cdot-}$, and/or RBD are shown in black.

(*48*, *49*). Results shown in Figure 5A also indicate that a small fraction of rhodamine-labeled Ras binds the RBD, because a slight increase in Ras rhodamine fluorescence was observed when GDP-bound rhodamine-labeled Ras is incubated with GTP for 30 min in the absence of $O_2^{\cdot-}$ or NO/O_2. This result suggests that only a minor fraction of the available RBD binds to the active GTP-bound form of Ras in the absence of $O_2^{\cdot-}$ or NO/O_2. When GDP-bound rhodamine-labeled Ras was treated with $O_2^{\cdot-}$ in the presence of GTP for 30 min prior to titration with the Raf-1-RBD, Ras-bound rhodamine fluorescence increased (Figure 5B), indicating that $O_2^{\cdot-}$ enhances Ras GDP GNE with GTP to populate the biologically active GTP-bound state of Ras. However, as noted above, a larger fraction GTP exchanges with Ras-GDP in the presence of ascorbate. As a control, when rhodamine-labeled GDP-loaded Ras was treated with $O_2^{\cdot-}$ in the presence of GDP for 30 min, Ras-rhodamine fluorescence did not increase (Figure 5B). Results from this control experiment indicate that, although Ras-bound GDP can be exchanged with free GDP, the inactive GDP-bound form is present in both exchanged and unexchanged Ras and does not bind the Raf-RBD with appreciable affinity relative to Ras-GTP. Furthermore, given that the treatment of Ras with $O_2^{\cdot-}$ produces apo Ras (*20*) and $O_2^{\cdot-}$-treated Ras in the presence of GDP does not appreciably bind the Raf-1 RBD (Figure 2B), the apo Ras state does not bind the Raf-1 RBD with noticeable affinity, consistent with previous observations that mutants of Ras that populate the GDP-bound or apo state of Ras are not active in promoting downstream signaling of Ras (*50*). As shown in Figure 4, ascorbate largely enhances NO/O_2-treated Ras GTP (and GDP) association. In parallel, treatment of ascorbate with $O_2^{\cdot-}$-treated Ras in the presence of GTP is expected to increase Ras RBD-binding affinity. When ascorbate was added after the addition of RBD to $O_2^{\cdot-}$-treated Ras in the presence of GTP, Ras RBD-binding is largely enhanced (Figure 5B), indicating that $O_2^{\cdot-}$ in the presence of ascorbate greatly facilitates Ras GDP exchange with GTP to produce Ras-GTP bound to the Raf-RBD, consistent with previous results (*20*).

Results shown in Figure 5B also indicate that treatment of Ras-SNO with $O_2^{\cdot-}$ in the presence of GTP and ascorbate does not promote Raf-1 RBD binding. These results suggest that the sulfur atom of Ras, once S-nitrosylated, is insensitive to $O_2^{\cdot-}$, and thereby, $O_2^{\cdot-}$-mediated Ras GDP exchange with GTP does not occur, consistent with the results shown in Figure 1B. Identical results were obtained upon measuring binding interactions between the Raf-1 RBD and NO/O_2-treated Ras in the absence and presence of ascorbate (not shown).

DISCUSSION

Numerous *in vivo* and *in vitro* studies have now implicated redox agents in regulation of Ras superfamily GTPase-mediated signaling pathways (*7*−*15*, *17*, *51*, *52*). Results obtained in this study aid in delineating the molecular mechanism of Ras regulation by various RNS and ROS.

Mechanism of ROS- and RNS-Mediated Ras GNE. H_2O_2 alone does not facilitate Ras guanine nucleotide dissociation (*20*). However, results from this study show that, in the presence of transition metals, H_2O_2 can facilitate Ras guanine nucleotide dissociation. The primary redox-active species that promotes Ras guanine nucleotide dissociation upon treatment of Ras with H_2O_2/transition metals or $ONOO^-$ appears to be $O_2^{\cdot-}$ and $^{\cdot}NO_2$, respectively. Because upregulation of K-Ras activity has been shown to lead to enhanced Cox-2 expression (*34*), it is intriguing to speculate that Cox-2-

produced H_2O_2 can be converted into $O_2^{\cdot-}$ (because cells contain various transition metals), which may reversibly regulate the activity of K-Ras via a feedback mechanism.

Results from these studies also indicate that a small fraction of $OH^{\cdot}$ generated in reaction mixtures containing H_2O_2/transition metals and $ONOO^-$ enhance Ras guanine nucleotide dissociation. Because the redox potential of $OH^{\cdot}$ is high (*21*), $OH^{\cdot}$ can react with a multitude of cellular components with little specificity. Thus, various protective measures may be employed by cells to reduce the levels of $OH^{\cdot}$. For example, catalase may facilitate the conversion of H_2O_2 into H_2O and O_2 (*53*) to prevent the generation of $OH^{\cdot}$ that may be cytotoxic if present at high enough concentrations (*26*). Moreover, if $OH^{\cdot}$ is formed, natural spin-trapping agents such as ascorbate and tocopherol (*54*) may quench $OH^{\cdot}$, leading to redox inactivation.

In the presence of CO_2, $ONOO^-$ decomposes rapidly to form $CO_3^{\cdot-}$ and $^{\cdot}NO_2$ (*23*). The concentration of CO_2 *in vivo* may be significant, because of high levels of bicarbonate in intracellular and intestinal fluids (*23*). Our kinetic and MS results obtained on Ras protein samples treated with $ONOO^-/CO_2$ indicate that $CO_3^{\cdot-}$ indeed facilitates Ras guanine nucleotide dissociation. Therefore, $CO_3^{\cdot-}$, in addition to $^{\cdot}NO_2$ and $O_2^{\cdot-}$, may play a role in the regulation of redox-active GTPases.

Among these identified redox agents (i.e., $^{\cdot}NO_2$, $O_2^{\cdot-}$, and $CO_3^{\cdot-}$), $O_2^{\cdot-}$ possesses the lowest redox potential [$\sim$0.9 V versus NHE (*24*)]. However, the estimated Ras guanine nucleotide dissociation rates facilitated by these redox agents are virtually similar. Therefore, the redox potential of Ras-$Cys^{118\cdot}$ may be lower that $\sim$0.9 V versus NHE, and thus, any redox agent that possesses a higher redox potential than $\sim$0.9 V versus NHE may be able to react with Ras-Cys^{118} thiol to produce a redox-active Ras-$Cys^{118\cdot}$.

Implication of Redox-Active Rho GTPase GNE by Various Redox Agents. We have recently shown that several Rho GTPase (i.e., Rac1, RhoA, and Cdc42) family members are redox-active and, like Ras, $^{\cdot}NO_2$ or $O_2^{\cdot-}$ facilitates guanine nucleotide dissociation (*47*). Even though the redox motif in Rho GTPases (Cys^{18}, Rac1 numbering) differs from Ras (Ras Cys^{118}), the mechanistic steps and process of ROS- and RNS-mediated GNE appear similar (*47*). Therefore, in addition to Ras, $ONOO^-$ (mainly via $^{\cdot}NO_2$) and $CO_3^{\cdot-}$ may facilitate the guanine nucleotide dissociation of the Rho GTPases. We have also shown that H_2O_2, in the presence of transition metals, facilitates Rho GTPase guanine nucleotide dissociation and proposed that H_2O_2/transition-metal-derived $OH^{\cdot}$ may play a key role in the process (*47*). However, given the results presented herein, the main redox-active species in the reaction mixture of H_2O_2 and transition metals is most likely $O_2^{\cdot-}$ rather than $OH^{\cdot}$, suggesting that the enhanced rate of guanine nucleotide dissociation for redox-active Rho GTPases by H_2O_2 in the presence of transition metals is mainly driven by $O_2^{\cdot-}$.

Redox-Mediated Ras Activation. Prolonged incubation of $^{\cdot}NO_2$ or $O_2^{\cdot-}$ with Ras in the presence of GTP (i.e., 30 min) but in the absence of a radical-quenching agent primarily induces the formation of an inactive apo Ras state, because only a small fraction of the available Ras is present as Ras GTP. These results imply that redox agents can serve to terminate Ras signaling (and other redox-active GTPases) by promoting the fast release of GDP or GTP from Ras to produce an inactive apo Ras state, which cannot undergo Ras GNE in the absence of a radical scavenger. A radical scavenger may then be necessary to recover the state of inactive apo Ras into a GTP-binding form of Ras. Consistent with this premise, efficient *in vitro* GTP reassociation can be observed in the presence of a radical-quenching agent to produce an active GTP-bound Ras, which, in turn, promotes the binding of Ras to the Ras-binding domain of Raf-1.

These results provide further support that $^{\cdot}NO_2$ and $O_2^{\cdot-}$ can promote Ras guanine nucleotide dissociation *in vivo* but may need to act in conjunction with radical-scavenging agents to promote Ras activation in cells. In animal and plant cells, GSH- and thiol-containing biomolecules are present at high levels and may function as radical-scavenging agents (*55*, *56*). The natural radical-quenching agent, ascorbate, may also serve as an additional radical-scavenging agent in cells (*54*). NO may also serve as a radical quencher, because it reacts with apo Ras-$Cys^{118\cdot}$ to produce Ras-SNO (*18*, *19*). Intriguingly, as shown in this study, Ras-SNO does not react with $^{\cdot}NO_2$ or $O_2^{\cdot-}$, indicating that, perhaps, the formation of Ras-SNO may render Ras insensitive to these redox agents *in vivo*. Similar to Ras, the redox-active Cys^{18} side chain of Rho GTPases can be S-nitrosylated (Rho-SNO) (*47*). Therefore, similar to Ras-SNO, S-nitrosylation of Rho GTPases may render the redox-active thiol insensitive to $^{\cdot}NO_2$- and $O_2^{\cdot-}$-mediated redox regulation. It is also possible that glutaredoxin (*57*) or the highly abundant peptide, glutathione (*55*, *56*), may be involved in cellular denitrosylation processes.

ACKNOWLEDGMENT

We thank MinQi Lu for the preparation of protein samples used in this study. We also thank Drs. Marcelo Bonini and Ronald Mason for helpful discussions. This work was supported by NIH Grants RO1 GM075431-01A1 (to S. L. C. and J. H.), RO1 CA89614-O1A1 (to S. L. C.), and PO1 HL45100 (to S. L. C.).

REFERENCES

1. Campbell, S. L., Khosravi-Far, R., Rossman, K. L., Clark, G. J., and Der, C. J. (1998) Increasing complexity of Ras signaling, *Oncogene 17*, 1395−1413.
2. Cox, A. D., and Der, C. J. (2003) The dark side of Ras: Regulation of apoptosis, *Oncogene 22*, 8999−9006.
3. Chong, H., Vikis, H. G., and Guan, K. L. (2003) Mechanisms of regulating the Raf kinase family, *Cell Signal 15*, 463−469.
4. Repasky, G. A., Chenette, E. J., and Der, C. J. (2004) Renewing the conspiracy theory debate: Does Raf function alone to mediate Ras oncogenesis? *Trends Cell Biol. 14*, 639−647.
5. Irani, K., and Goldschmidt-Clermont, P. (1998) Ras, superoxide, and signal transduction, *Biochem. Pharmacol. 55*, 1339−1346.
6. Geyer, M., and Wittinghofer, A. (1997) GEFs, GAPs, GDIs, and effectors: Taking a closer (3D) look at the regulation of Ras-related GTP-binding proteins, *Curr. Opin. Struct. Biol. 7*, 786−792.
7. Adachi, T., Pimentel, D. R., Heibeck, T., Hou, X., Lee, Y. J., Jiang, B., Ido, Y., and Cohen, R. A. (2004) S-Glutathiolation of Ras mediates redox-sensitive signaling by angiotensin II in vascular smooth muscle cells, *J. Biol. Chem. 279*, 29857−29862.
8. Baker, T., Booden, M., and Buss, J. (2000) S-Nitrosocysteine increases palmitate turnover on Ha-Ras in NIH 3T3 cells, *J. Biol. Chem. 275*, 22037−22047.
9. Lander, H. M., Hajjar, D. P., Hempstead, B. L., Mirza, U. A., Chait, B. T., Campbell, S. L., and Quilliam, L. A. (1997) A molecular redox switch on $p21^{Ras}$. Structural basis for the nitric oxide−$p21^{Ras}$ interaction, *J. Biol. Chem. 272*, 4323−4326.
10. Lander, H. M., Ogiste, J. S., Pearce, S. F., Levi, R., and Novogrodsky, A. (1995) Nitric oxide-stimulated guanine nucleotide exchange on $p21^{Ras}$, *J. Biol. Chem. 270*, 7017−7020.

11. Mitsushita, J., Lambeth, J. D., and Kamata, T. (2004) The superoxide-generating oxidase Nox1 is functionally required for Ras oncogene transformation, *Cancer Res. 64*, 3580−3585.
12. Chuang, J. I., Chang, T. Y., and Liu, H. S. (2003) Glutathione depletion-induced apoptosis of Ha-ras-transformed NIH3T3 cells can be prevented by melatonin, *Oncogene 22*, 1349−1357.
13. Nimnual, A. S., Taylor, L. J., and Bar-Sagi, D. (2003) Redox-dependent downregulation of Rho by Rac, *Nat. Cell Biol. 5*, 236−241.
14. Dawson, T. M., Sasaki, M., Gonzalez-Zulueta, M., and Dawson, V. L. (1998) Regulation of neuronal nitric oxide synthase and identification of novel nitric oxide signaling pathways, *Prog. Brain Res. 118*, 3−11.
15. Gonzalez-Zulueta, M., Feldman, A. B., Klesse, L. J., Kalb, R. G., Dillman, J. F., Parada, L. F., Dawson, T. M., and Dawson, V. L. (2000) Requirement for nitric oxide activation of $p21^{Ras}$/extracellular regulated kinase in neuronal ischemic preconditioning, *Proc. Natl. Acad. Sci. U.S.A. 97*, 436−441.
16. Lander, H. M., Milbank, A. J., Tauras, J. M., Hajjar, D. P., Hempstead, B. L., Schwartz, G. D., Kraemer, R. T., Mirza, U. A., Chait, B. T., Burk, S. C., and Quilliam, L. A. (1996) Redox regulation of cell signalling, *Nature 381*, 380−381.
17. Mittar, D., Sehajpal, P. K., and Lander, H. M. (2004) Nitric oxide activates Rap1 and Ral in a Ras-independent manner, *Biochem. Biophys. Res. Commun. 322*, 203−209.
18. Heo, J., and Campbell, S. L. (2004) Mechanism of $p21^{Ras}$ S-nitrosylation and kinetics of nitric oxide-mediated guanine nucleotide exchange, *Biochemistry 43*, 2314−2322.
19. Heo, J., Prutzman, K. C., Mocanu, V., and Campbell, S. L. (2005) Mechanism of free radical nitric oxide-mediated Ras guanine nucleotide dissociation, *J. Mol. Biol. 346*, 1423−1440.
20. Heo, J., and Campbell, S. L. (2005) Superoxide anion radical modulates the activity of Ras and Ras-related GTPases by a radical-based mechanism similar to that of nitric oxide, *J. Biol. Chem. 280*, 12438−12445.
21. Augusto, O., Bonini, M. G., Amanso, A. M., Linares, E., Santos, C. C., and de Menezes, S. L. (2002) Nitrogen dioxide and carbonate radical anion: Two emerging radicals in biology, *Free Radical Biol. Med. 32*, 841−859.
22. Bonaventura, C., Ferruzzi, G., Tesh, S., and Stevens, R. (1999) Effects of S-nitrosation on oxygen binding by normal and sickle cell hemoglobin, *J. Biol. Chem. 274*, 24742−24748.
23. Goldstein, S., Lind, J., and Merenyi, G. (2005) Chemistry of peroxynitrites as compared to peroxynitrates, *Chem. Rev. 105*, 2457−2470.
24. Stubbe, J., and van der Donk, W. A. (1998) Protein radicals in enzyme catalysis, *Chem. Rev. 98*, 705−762.
25. Bonini, M. G., Radi, R., Ferrer-Sueta, G., Ferreira, A. M., and Augusto, O. (1999) Direct EPR detection of the carbonate radical anion produced from peroxynitrite and carbon dioxide, *J. Biol. Chem. 274*, 10802−10806.
26. Wardman, P., and Candeias, L. P. (1996) Fenton chemistry: An introduction, *Radiat. Res. 145*, 523−531.
27. Bielski, B. H., and Gebicki, J. M. (1974) Study of peroxidase mechanisms by pulse radiolysis. 3. The rate of reaction of O_2^- and HO_2 radicals with horesradish peroxidase compound I, *Biochim. Biophys. Acta 364*, 233−235.
28. Khan, A. U., and Kasha, M. (1994) Singlet molecular oxygen in the Harber−Weiss reaction, *Proc. Natl. Acad. Sci. U.S.A. 91*, 12365−12367.
29. Forstermann, U., and Kleinert, H. (1995) Nitric oxide synthase: Expression and expressional control of the three isoforms, *Naunyn-Schmiedeberg's Arch. Pharmacol. 352*, 351−364.
30. Xia, Y., Roman, L. J., Masters, B. S., and Zweier, J. L. (1998) Inducible nitric-oxide synthase generates superoxide from the reductase domain, *J. Biol. Chem. 273*, 22635−22639.
31. Millar, T. M., Stevens, C. R., and Blake, D. R. (1997) Xanthine oxidase can generate nitric oxide from nitrate in ischaemia, *Biochem. Soc. Trans. 25*, 528S.
32. Zhang, Z., Naughton, D. P., Blake, D. R., Benjamin, N., Stevens, C. R., Winyard, P. G., Symons, M. C., and Harrison, R. (1997) Human xanthine oxidase converts nitrite ions into nitric oxide (NO), *Biochem. Soc. Trans. 25*, 524S.
33. Hodges, G. R., Young, M. J., Paul, T., and Ingold, K. U. (2000) How should xanthine oxidase-generated superoxide yields be measured? *Free Radical Biol. Med. 29*, 434−441.
34. Maciag, A., and Anderson, L. M. (2005) Reactive oxygen species and lung tumorigenesis by mutant K-ras: A working hypothesis, *Exp. Lung Res. 31*, 83−104.
35. Hille, R., and Nishino, T. (1995) Flavoprotein structure and mechanism. 4. Xanthine oxidase and xanthine dehydrogenase, *FASEB J. 9*, 995−1003.
36. Bokoch, G. M., and Knaus, U. G. (2003) NADPH oxidases: Not just for leukocytes anymore! *Trends Biochem. Sci. 28*, 502−508.
37. Lander, H. M., Ogiste, J. S., Teng, K. K., and Novogrodsky, A. (1995) $p21^{Ras}$ as a common signaling target of reactive free radicals and cellular redox stress, *J. Biol. Chem. 270*, 21195−21198.
38. Campbell-Burk, S. L., and Carpenter, J. W. (1995) Refolding and purification of Ras proteins, *Methods Enzymol. 255*, 3−13.
39. Reinstein, J., Schlichting, I., Frech, M., Goody, R. S., and Wittinghofer, A. (1991) p21 with a phenylalanine 28 → leucine mutation reacts normally with the GTPase activating protein GAP but nevertheless has transforming properties, *J. Biol. Chem. 266*, 17700−17706.
40. Bradford, M. M. (1976) A rapid and sensitive method for the quantitation of microgram quantities of protein utilizing the principle of protein−dye binding, *Anal. Biochem. 72*, 248−254.
41. Olojo, R. O., Xia, R. H., and Abramson, J. J. (2005) Spectrophotometric and fluorometric assay of superoxide ion using 4-chloro-7-nitrobenzo-2-oxa-1,3-diazole, *Anal. Biochem. 339*, 338−344.
42. Steinman, H. M., Naik, V. R., Abernethy, J. L., and Hill, R. L. (1974) Bovine erythrocyte superoxide dismutase. Complete amino acid sequence, *J. Biol. Chem. 249*, 7326−7338.
43. Heo, J., Staples, C. R., Halbleib, C. M., and Ludden, P. W. (2000) Evidence for a ligand CO that is required for catalytic activity of CO dehydrogenase from *Rhodospirillum rubrum*, *Biochemistry 39*, 7956−7963.
44. Grossi, L., and Montevecchi, P. C. (2002) A kinetic study of S-nitrosothiol decomposition, *Chemistry 8*, 380−387.
45. Lenzen, C., Cool, R. H., Prinz, H., Kuhlmann, J., and Wittinghofer, A. (1998) Kinetic analysis by fluorescence of the interaction between Ras and the catalytic domain of the guanine nucleotide exchange factor $Cdc25^{Mm}$, *Biochemistry 37*, 7420−7430.
46. Aikens, J., and Dix, T. A. (1991) Perhydroxyl radical (HOO•) initiated lipid peroxidation. The role of fatty acid hydroperoxides, *J. Biol. Chem. 266*, 15091−15098.
47. Heo, J., and Campbell, S. L. (2005) Mechanism of redox-mediated guanine nucleotide exchange on redox-active Rho GTPases, *J. Biol. Chem. 280*, 31003−31010.
48. Herrmann, C., Martin, G. A., and Wittinghofer, A. (1995) Quantitative analysis of the complex between $p21^{Ras}$ and the Ras-binding domain of the human Raf-1 protein kinase, *J. Biol. Chem. 270*, 2901−2905.
49. Sydor, J. R., Engelhard, M., Wittinghofer, A., Goody, R. S., and Herrmann, C. (1998) Transient kinetic studies on the interaction of Ras and the Ras-binding domain of c-Raf-1 reveal rapid equilibration of the complex, *Biochemistry 37*, 14292−14299.
50. Stewart, S., and Guan, K. L. (2000) The dominant negative Ras mutant, N17Ras, can inhibit signaling independently of blocking Ras activation, *J. Biol. Chem. 275*, 8854−8862.
51. Mott, H. R., Carpenter, J. W., and Campbell, S. L. (1997) Structural and functional analysis of a mutant Ras protein that is insensitive to nitric oxide activation, *Biochemistry 36*, 3640−3644.
52. Yun, H. Y., Gonzalez-Zulueta, M., Dawson, V. L., and Dawson, T. M. (1998) Nitric oxide mediates *N*-methyl-D-aspartate receptor-induced activation of $p21^{Ras}$, *Proc. Natl. Acad. Sci. U.S.A. 95*, 5773−5778.
53. Vainshtein, B. K., Melik-Adamyan, W. R., Barynin, V. V., Vagin, A. A., and Grebenko, A. I. (1981) Three-dimensional structure of the enzyme catalase, *Nature 293*, 411−412.
54. Buettner, G. R. (1993) The pecking order of free radicals and antioxidants: Lipid peroxidation, α-tocopherol, and ascorbate, *Arch. Biochem. Biophys. 300*, 535−543.
55. Stamler, J. S., Jaraki, O., Osborne, J., Simon, D. I., Keaney, J., Vita, J., Singel, D., Valeri, C. R., and Loscalzo, J. (1992) Nitric oxide circulates in mammalian plasma primarily as an S-nitroso adduct of serum albumin, *Proc. Natl. Acad. Sci. U.S.A. 89*, 7674−7677.
56. Heo, J., and Holbrook, G. (1999) Regulation of 2-carboxy-D-arabinitol 1-phosphate phosphatase: Activation by glutathione and interaction with thiol reagents, *Biochem. J. 338*, 409−416.
57. Shelton, M. D., Chock, P. B., and Mieyal, J. J. (2005) Glutaredoxin: Role in reversible protein S-glutathionylation and regulation of redox signal transduction and protein translocation, *Antioxid. Redox Signaling 7*, 348−366.
58. Zang, L. V., and Shi, X. (1995) Evidence for superoxide radical production in peroxynitrite decomposition, *Biochem. Mol. Biol. Int. 37*, 355−360.

BI051872M